Developing systems for high-throughput screening of infectious diseases using zebrafish

Veneman, W.J.

Chapter 6

Distribution of micro and nano range sized biomaterials after yolk injection into zebrafish larvae

Wouter J. Veneman[1,2], Martina G. Vijver[2], Annemarie H. Meijer[1], Herman P. Spaink[1]

[1]Institute of Biology Leiden, Leiden University
[2]Institute of Environmental Sciences, Leiden University

Manuscript in preparation

Abstract

Biomaterial-associated infection is a major problem in modern medicine. The presence of foreign body materials such as artificial hips or intravenous needles can in combination with the normally innocent skin bacterium, *Staphylococcus epidermidis* cause infections that are difficult to treat. To test and develop new compositions that could be used as biomaterials we developed a screening method. Here we report the outcome of a variety of nanometer and micrometer sized biomaterials injected into the zebrafish embryos. We found a size depended outcome of the polystyrene biomaterial distribution throughout the embryo. These results could hopefully contribute to the early stage of development of biocompatible materials for modern medicine.

Introduction

Thanks to modern medicine, the past decades people have a longer life expectation and their physical condition can be improved up to old age, since it is easier to replace body parts such bones or cartilage. However, the risk of the accompanying surgical treatments lead to a great chance of infection due to the implantation of the used biomaterial/biomedical devices such as an artificial hips, intravenous needles or catheters. These biomaterial-associated infections (BAI) are mainly caused by the skin bacterium *Staphylococcus epidermidis* [1-4]. This means that there is a great demand for biomaterials and medical devices that are biocompatible in such a way that it does not get rejected by the human body but also does not induce infections.

In previous studies we already showed that the zebrafish embryo is a versatile model to study the pathogenesis of *S. epidermidis* [5, 6]. The use of zebrafish larvae as whole vertebrate animal model in modern research has been well established. The larvae have great *in vivo* imaging potential due to their transparency and the large amount of transgenic strains expressing fluorescent proteins [7-9]. Secondly they are very well suited for high-throughput screening since zebrafish are relatively cheap to house, the eggs can be obtained in large amounts in a single time, and solutions containing DNA, RNA, morpholinos and pathogens can be introduced robotically [10, 11]. Furthermore, the analysis of these injected embryos can be followed over time using automated screening methods [5]. All these advantages have led to the fact that many human diseases such as tuberculosis, cancer, and cardiovascular defects have been modelled using zebrafish larvae [12-20].

In order to develop a screening model for BAI using zebrafish we report in this paper the outcome of distribution of biomaterials after injection. For this we used a set of fluorescently labelled polystyrene particles with a diameter ranging from 15 micrometer to 70 nanometer. Our first strategy was to inject particles as large as possible, so that these would not get phagocytized, but still be small enough to be injected easily using glass micro capillaries. The second strategy was to inject nanometer sized particles,

since these will probably spread easier due to their phagocytosis by motile immune cells, and could therefore provide more details about the distribution pattern of how injected agents would behave. We mainly chose the yolk of eggs between the 16 and 256 cell stage as injection site, so results would be comparable with earlier reports of injection of *S. epidermidis* into the yolk. Secondly this method can easily be automated for future experiments or large high-throughput screens.

Material and methods

Zebrafish husbandry

Zebrafish were handled in compliance with animal welfare regulations and maintained according to standard protocols (http://ZFIN.org). Embryos were grown at 28°C in egg water (60 µg/ml Instant ocean sea salt, Sera Marin). The egg water was refreshed every day.

Experimental design

Injections were performed using mixed egg clutches from the *Tg(bactin:Hras-EGFP VU119)* [21] strain. For yolk injections: eggs were staged between 16 and 128 cell stage by morphological criteria, and injected into the yolk with 1 nl of 4% polyvinylpyrrolidone$_{40}$ (PVP_{40}) containing 5 mg/ml nanometer or micrometer particles (see table 1). For tail muscle injection: 2 and 3 day old larvae were staged by morphological criteria and anaesthetized (0.02% buffered 3-aminobenzoic acid ethyl ester (Tricaine, Sigma) in egg water). Larvae were injected into the tail muscle [22] with approximately 1-10 nl containing one particle. Injections were controlled using a Leica M50 stereomicroscope together with a FemtoJet micro-injector (Eppendorf) and a micromanipulator with pulled and bevelled micro capillary needles.

Table 1: commercial available nanometer and micrometer sized particles as used in the experiments. nm= nanometer, µm= micrometer

Size	Composition	Fluorescence dye	Manufacture	Reference number
70 nm	Polystyrene	Nile red	Corpuscular inc. (USA)	103125-05
250 nm	Polystyrene	Nile red	Corpuscular inc. (USA)	103127-05
2.2 µm	Polystyrene	Nile red	Corpuscular inc. (USA)	103235-05
4.2 µm	Polystyrene	Nile red	Corpuscular inc. (USA)	103129-05
9.9 µm	Polystyrene	Nile red	Corpuscular inc. (USA)	103245-05
15 µm	Polystyrene	Nile red	Corpuscular inc. (USA)	103251-05

Microscopy

Embryos were examined and imaged daily using a fluorescence stereo microscope (MZ 205 FA, Leica). Embryos were kept under anaesthesia (0.02% buffered 3-aminobenzoic acid ethyl ester (Tricaine, Sigma) in egg water) during imaging. The image processing package Fiji [23] was used for processing and analysis of the images.

Results and discussion

We used a set of polystyrene particles as proof of principle for studying the distribution of injected biomaterials into embryos. These polystyrene particles are chosen as they are commercially available in a monodispersed form in many different sizes. Earlier biomaterial injection experiments with materials that are more related to medical devices such as titanium, poly(lactic-co-glycolic acid) or polycaprolactone led to difficulties. These particles are irregular in shape as well size, with as result clogging of the glass micro capillaries and inconsistent outcomes. However, with the monodispersed polystyrene particles these problems did not occur. Using a 4% PVP_{40} solution as a carrier made it possible to inject polystyrene particles into the embryonic yolk because the viscosity of the solvent prevented the particles from flowing out after injection. The visualization of the distribution of particles was facilitated by the use of the *Tg(bactin:Hras-EGFP VU119)* strain which expresses membrane-targeted GFP as shown in Figure 1 and 2. Following injection into the yolk of 16-128 cell stage embryos, we observed a difference in the distribution of biomaterials of various sizes throughout the body of the embryo (Figure 3). The nanometer sized biomaterials spread more compared to the micrometer sized biomaterials. One possible explanation could be that the concentration of particles per nanoliter of the small particles was higher since all suspensions were diluted to a 5 mg/ml concentration and the same volume of materials was injected. Another explanation could be that there is indeed a size dependent factor, which makes that the smaller beads spread easier than larger sized beads. This is in line with earlier findings of Desai et al. (1996 & 1997) [24, 25], who also found that nanometer sized particles had a higher uptake in rat tissue and *in vitro* compared to the micrometer sized particles. We did find that the smaller sized particles (70 & 250 nm) accumulate around the heart region at 3 to 4 days post injection (dpi) (Figure 2) from where they probably distribute throughout the body. In a few experiments we found a very small number of embryos with larger sized beads (≥ 9.9 μm) throughout the body. Since the embryos did not show any signs of distributed particles yet at 1 day post fertilization (dpf), we can rule out the possibility that the yolk-injected particles were spread as a result of uptake by cells during the first hours of development, as in the case with early RNA or DNA injections before the 16 cell stage. It is also unlikely that these large particles were distributed at later developmental stages via the vasculature, since the maximum diameter of the vasculature is also around 10 μm in diameter. We performed a whole mount L-plastin immunohistochemistry [26] on larvae injected with the larger sized particles (≥ 9.9 μm) to check for possible uptake by leukocytes at later stages from 2 until 5 dpi, but we could not colocalize the particles with leukocytes throughout the body (data not shown).

Even though the percentage of embryos showing a distribution of particles through the body is low, it indicates that it is possible for such materials being taken up into the body of the embryo after injection into the yolk. This has implications for the results of earlier reports [5, 6, 10, 11] on spreading of bacteria and human cancer cells after

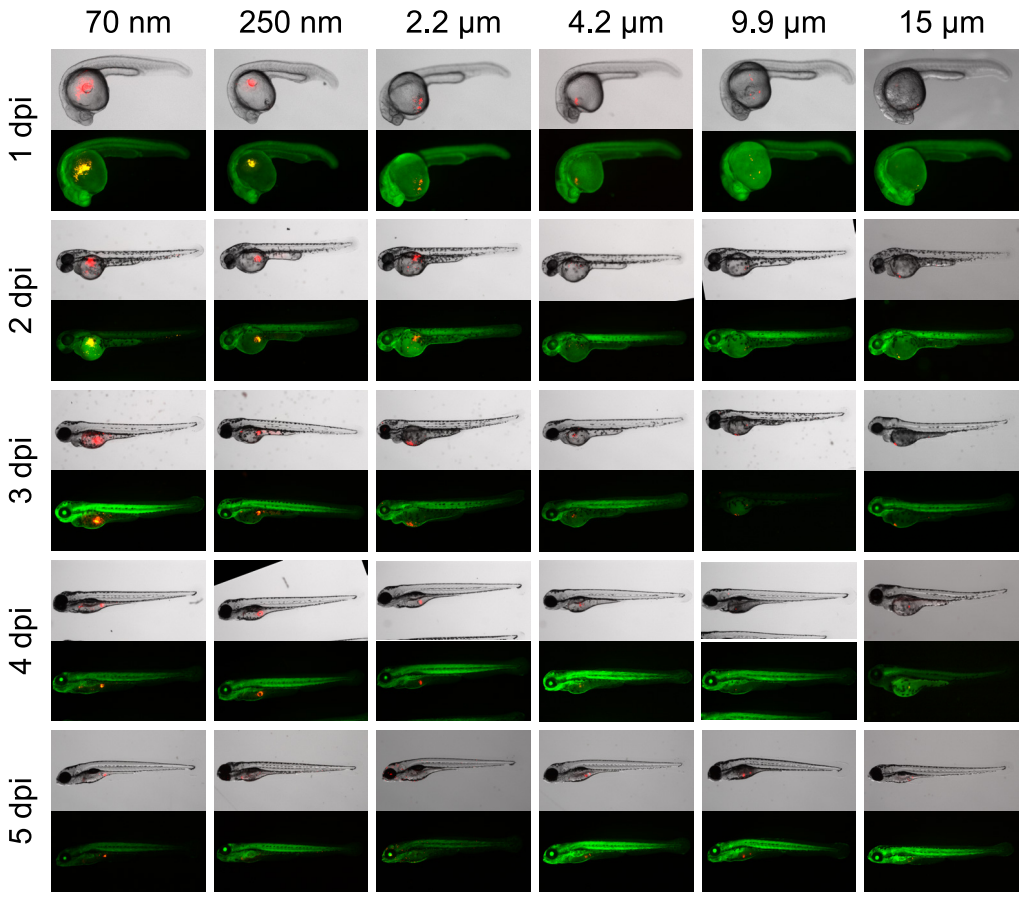

Figure 1: Representative bright field /fluorescence overlay images showing migration of Nile red fluorescence particles throughout the *Tg(bactin:Hras-EGFP VU119)* embryos over a 5 day period. The x axis shows the different sizes of particles injected and the y axis shows the time period from 1 until 5 dpi.

being injected into the early embryonic yolk since it indicates that distribution could be driven by unknown aspecific processes from the host. We are hoping to unravel the mechanism(s) of such aspecific transport from yolk to body in future research.

All previously described experiments were based on the yolk injection method. We also performed injections of beads in the tail muscle of 2 and 3 day old larvae, which mimics the implantation of an artificial implant in human chirurgical applications, since the implantation is performed directly into tissue. However, when using the 9.9 µm sized particles these injections proved to be very labour intensive, and did not result in the biomaterial to remain in the same place after injection (data not shown). In almost all cases the particles were pushed out of the tissue while injecting. Even when the particle would stay at the implantation side, a considerable amount of tissue damage occurred.

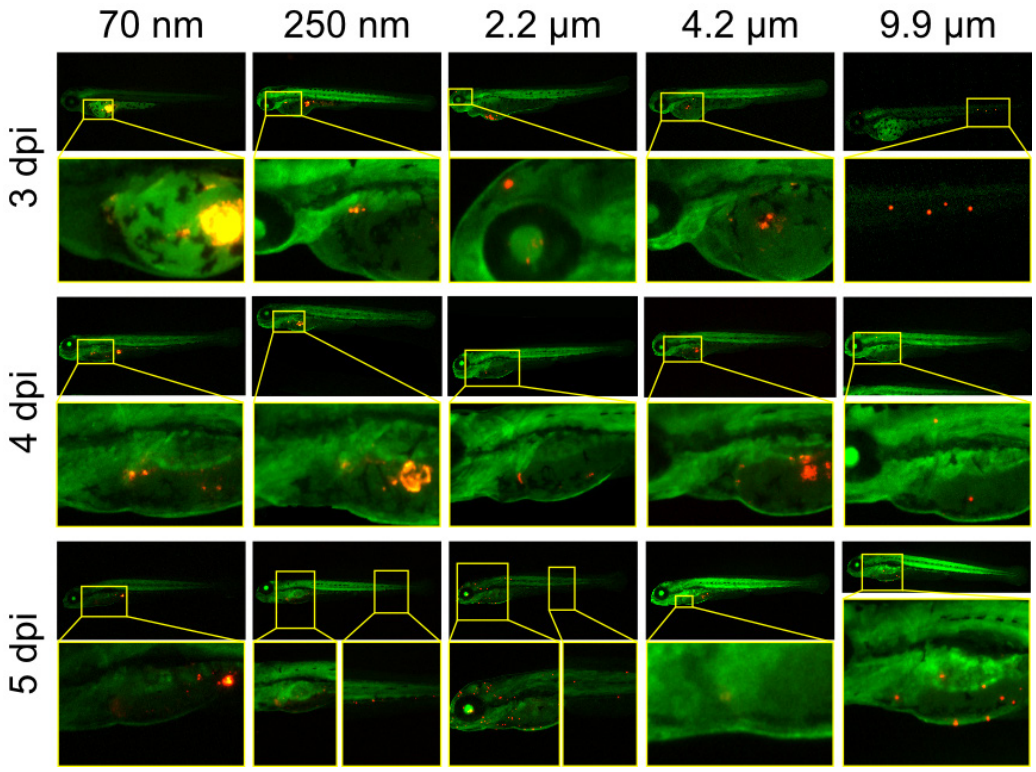

Figure 2: Detailed images of *Tg(bactin:Hras-EGFP VU119)* larvae injected with particles. The yellow boxes show the particles close to the heart region or already migrated away from the yolk injection side.

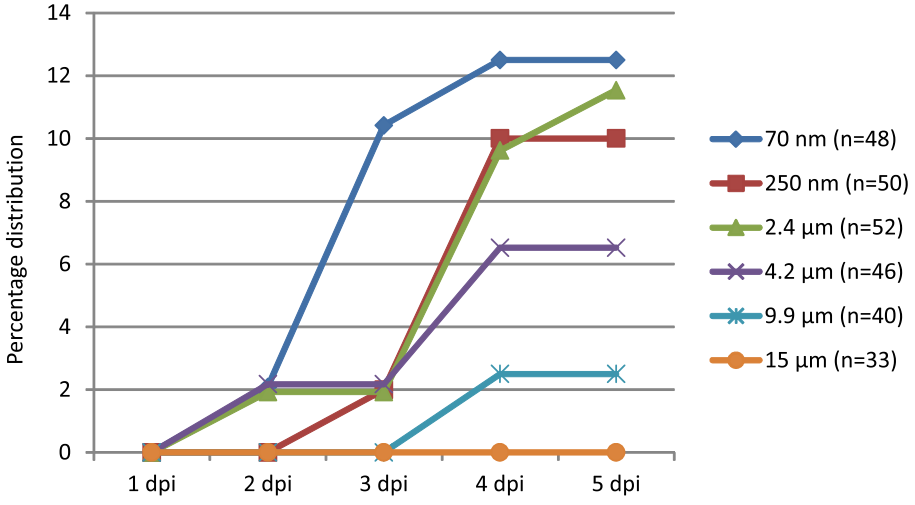

Figure 3: Quantification of distributed particles. The graph shows the percentage of embryos with nano or micrometer sized beads that were spread away from the yolk injection side at subsequent dpi.

Conclusions

We found that there was a difference based on size in distribution of biomaterials. The preferable larger sized biomaterials (≥ 9.9 μm) migrated less than the smaller sized biomaterials (≤ 2.2 μm). The location where they accumulate still remains unknown, however if they spread, such as the smaller particles (≥ 2.2 μm), it probably starts at the heart region from where they distribute out inside the body. The mechanism of how particles spread also remains unknown, however we think that the larger (≥ 9.9 μm) particles do not get taken up by leucocytes and there is no evidence for spreading via the vasculature. Nevertheless we hope to find the mechanisms/processes that are involved during the migration of these particles in the future.

Acknowledgements

We would like to thank Oliver Stockhammer, Xiaolin Zhang and Bas Zaat (AMC) for their help with biomaterial implantations, Davy de Witt and Ulrike Nehrdich for fish caretaking, Paul Martin (University of Bristol) for L-plastin antibody. This research forms part of the Project P5.03 IBIZA of the research program of the BioMedical Materials institute, co-funded by the Dutch Ministry of Economic Affairs. M.G. Vijver is granted via NWO VIDI no. 864.13.010.

References

1. Broekhuizen CA, Schultz MJ, van der Wal AC, Boszhard L, de Boer L, Vandenbroucke-Grauls CM, Zaat SA: Tissue around catheters is a niche for bacteria associated with medical device infection. Crit Care Med 2008, 36(8):2395-2402.

2. Busscher HJ, van der Mei HC, Subbiahdoss G, Jutte PC, van den Dungen JJ, Zaat SA, Schultz MJ, Grainger DW: Biomaterial-associated infection: locating the finish line in the race for the surface. Sci Transl Med 2012, 4(153):153rv110.

3. Zaat S, Broekhuizen C, Riool M: Host tissue as a niche for biomaterial-associated infection. Future Microbiol 2010, 5(8):1149-1151.

4. Boelens JJ, Dankert J, Murk JL, Weening JJ, van der Poll T, Dingemans KP, Koole L, Laman JD, Zaat SA: Biomaterial-associated persistence of Staphylococcus epidermidis in pericatheter macrophages. J Infect Dis 2000, 181(4):1337-1349.

5. Veneman WJ, Marin-Juez R, de Sonneville J, Ordas A, Jong-Raadsen S, Meijer AH, Spaink HP: Establishment and optimization of a high throughput setup to study Staphylococcus epidermidis and Mycobacterium marinum infection as a model for drug discovery. J Vis Exp 2014(88):e51649.

6. Veneman WJ, Stockhammer OW, de Boer L, Zaat SA, Meijer AH, Spaink HP: A zebrafish high throughput screening system used for Staphylococcus epidermidis infection marker discovery. BMC Genomics 2013, 14:255.

7. Brittijn SA, Duivesteijn SJ, Belmamoune M, Bertens LF, Bitter W, de Bruijn JD, Champagne DL, Cuppen E, Flik G, Vandenbroucke-Grauls CM et al: Zebrafish development and regeneration: new tools for biomedical research. Int J Dev Biol 2009, 53(5-6):835-850.

8. Meijer AH, Spaink HP: Host-pathogen interactions made transparent with the zebrafish model. Curr Drug Targets 2011, 12(7):1000-1017.

9. Meijer AH, van der Vaart M, Spaink HP: Real-time imaging and genetic dissection of host-microbe interactions in zebrafish. Cell Microbiol 2014, 16(1):39-49.

10. Carvalho R, de Sonneville J, Stockhammer OW, Savage ND, Veneman WJ, Ottenhoff TH, Dirks RP, Meijer AH, Spaink HP: A high-throughput screen for tuberculosis progression. PLoS One 2011, 6(2):e16779.

11. Spaink HP, Cui C, Wiweger MI, Jansen HJ, Veneman WJ, Marin-Juez R, de Sonneville J, Ordas A, Torraca V, van der Ent W et al: Robotic injection of zebrafish embryos for high-throughput screening in disease models. Methods 2013, 62(3):246-254.

12. Lieschke GJ, Currie PD: Animal models of human disease: zebrafish swim into view. Nat Rev Genet 2007, 8(5):353-367.

13. Cronan MR, Tobin DM: Fit for consumption: zebrafish as a model for tuberculosis. Dis Model Mech 2014, 7(7):777-784.

14. Tobin DM, Ramakrishnan L: Comparative pathogenesis of Mycobacterium marinum and Mycobacterium tuberculosis. Cell Microbiol 2008, 10(5):1027-1039.

15. van der Ent W, Jochemsen AG, Teunisse AF, Krens SF, Szuhai K, Spaink HP, Hogendoorn PC, Snaar-Jagalska BE: Ewing sarcoma inhibition by disruption of EWSR1-FLI1 transcriptional activity and reactivation of p53. J Pathol 2014, 233(4):415-424.

16. Amatruda JF, Patton EE: Genetic models of cancer in zebrafish. Int Rev Cell Mol Biol 2008, 271:1-34.

17. Etchin J, Kanki JP, Look AT: Zebrafish as a model for the study of human cancer. Methods Cell Biol 2011, 105:309-337.

18. Konantz M, Balci TB, Hartwig UF, Dellaire G, Andre MC, Berman JN, Lengerke C: Zebrafish xenografts as a tool for in vivo studies on human cancer. Ann N Y Acad Sci 2012, 1266:124-137.

19. Payne E, Look T: Zebrafish modelling of leukaemias. Br J Haematol 2009, 146(3):247-256.

20. Bakkers J: Zebrafish as a model to study cardiac development and human cardiac disease. Cardiovasc Res 2011, 91(2):279-288.

21. Cooper MS, Szeto DP, Sommers-Herivel G, Topezewski J, Solnica-Krezel L, Kang HC, Johnson I, Kimelman D: Visualizing morphogenesis in transgenic zebrafish embryos using BODIPY TR methyl ester dye as a vital counterstain for GFP. Dev Dynam 2005, 232(2):359-368.

22. Benard EL, van der Sar AM, Ellett F, Lieschke GJ, Spaink HP, Meijer AH: Infection of zebrafish embryos with intracellular bacterial pathogens. J Vis Exp 2012(61).

23. Schindelin J, Arganda-Carreras I, Frise E, Kaynig V, Longair M, Pietzsch T, Preibisch S, Rueden C, Saalfeld S, Schmid B et al: Fiji: an open-source platform for biological-image analysis. Nat Methods 2012, 9(7):676-682.

24. Desai MP, Labhasetwar V, Amidon GL, Levy RJ: Gastrointestinal uptake of biodegradable microparticles: Effect of particle size. Pharmaceut Res 1996, 13(12):1838-1845.

25. Desai MP, Labhasetwar V, Walter E, Levy RJ, Amidon GL: The mechanism of uptake of biodegradable microparticles in Caco-2 cells is size dependent. Pharmaceut Res 1997, 14(11):1568-1573.

26. Mathias JR, Dodd ME, Walters KB, Rhodes J, Kanki JP, Look AT, Huttenlocher A: Live imaging of chronic inflammation caused by mutation of zebrafish Hai1. J Cell Sci 2007, 120(Pt 19):3372-3383.